Pergamon

Bioorganic & Medicinal Chemistry, Vol. 5, No. 8, pp 1531–1541, 1997

PII: S0968-0896(97)00099-0
0968-0896/97 $17.00 + 0.00

Modulation of Human α-Thrombin Activity with Phosphonate Ester Inhibitors

Edith J. Enyedy and Ildiko M. Kovach*
The Catholic University of America, Department of Chemistry, Washington, DC 20064, U.S.A.

Abstract—Enantiomers of 4-nitrophenyl 4-X-phenacyl methylphosphonate esters (X = H, PMN; CH_3; and CH_3O) inactivate human α-thrombin with rate constants 4–235 M^{-1} s^{-1} in pH 6.5, 0.025 M citrate buffer, and 0.15 M NaCl at 7.0±0.1 °C. Stereoselectivity of the inactivation of thrombin is 2–39 and favors the levorotatory enantiomers. The pH-dependence of inactivation of thrombin by (−)-PMN is sigmoidal and consistent with the participation of a catalytic residue with a pK_a of 8.0±0.1 in 0.15 M NaCl and a pK_a of 7.4±0.2 in 0.15 M choline chloride in the nucleophilic attack of the catalytic Ser at phosphorus. The solvent isotope effect on k_i/K_i in the pH-independent region of the reaction is 2.26±0.17. Thrombin activity returns from the adducts on the 2–7 h time scale at 25.0±0.1 °C via a self-catalyzed intramolecular reaction. The pH dependence of reactivation is significant from the adduct formed with (−)-CH_3O-PMN and (−)-CH_3-PMN and less so from the adducts formed with the other enantiomers of the inhibitors. Kinetic p*K*s ~7.2, with the exception of the adducts with (−)-PMN and (−)-CH_3O-PMN, indicate that a pH-dependent conformational change affects the rate of dephosphonylation. A structural interpretation of the stereoselectivity and other mechanistic features is provided based on the energy-optimized structures of the adducts. Pharmaco-medical use of human α-thrombin covalently modified by the PMNs is suggested. © 1997 Elsevier Science Ltd.

Introduction

Human α-thrombin (EC 3.4.21.5) is a glycosylated trypsin-like serine protease formed towards the end of the blood coagulation cascade. Under physiological conditions, α-thrombin shows procoagulant as well as anticoagulant activities.[1] α-Thrombin binds and cleaves fibrinogen selectively at only four Arg-Gly sites out of 300 Arg-Xaa peptide bonds[2] to generate fibrin, which then assembles to form blood clots. When bound to thrombomodulin, α-thrombin functions as an anticoagulant by activating protein C[3] and stimulating endothelial cells to produce t-PA.[4] Thrombin also activates platelets and the blood coagulation factors V, VII, VIII, XI, and XIII.[5]

α-Thrombin is formed of two chains; A (36 residues, MW = 4600) and B (259 residues, MW = 32,000) linked together by a disulfide bond. Since the three-dimensional structure of α-thrombin was determined in 1989,[6,7] a wealth of information became available on the stereochemical set-up of the catalytic triad, Ser195, His57, and Asp102, the oxyanion hole and the unique binding components of the enzyme[8] that serve the diverse roles of thrombin. The B-insertion loop has a key role in screening out small and large effectors.[7,9] Interpretation of the function of thrombin with substrates and inhibitors can now be based on the structural details of the enzyme and some of its adducts.[7,10–13]

α-Thrombin is one of nature's most efficient catalysts of substrates that carry all elements of the specificity requirements of the enzyme. It also catalyzes the hydrolysis of esters and amides that can satisfy some binding preferences of the enzyme and has good leaving groups. A significant advancement in the understanding of thrombin catalysis was the discovery of allosteric regulation[14,15] by the flow of Na^+ ions that effect a conformational change between the 'fast' and 'slow' forms of the enzyme.[1,16–20] The 'fast' form promotes the hemostatic function while the 'slow' form promotes the thrombolytic function of thrombin.

Some of thrombin's natural inhibitors are hirudin, heparin, and antithrombin III.[6,21] Although therapeutic use of these has been explored, extensive efforts are now exerted in designing small molecular inhibitors of the enzyme as drugs.[21] Thrombin, as other serine proteases, is also uniquely sensitive to electrophilic inhibitors giving rise to covalent adducts of the enzyme that are considered transition state analogues.[22] The D-Phe-Pro-Arg chloromethyl-ketone (PPACK) adduct of thrombin[7,10] was the first of these for which an X-ray structure at 1.9 Å resolution had been determined. The transition state analogue concept[23] has been exploited in the design of tetracoordinate covalent adducts formed with boronate esters[13,24–26] and peptide-phosphonate ester inhibitors.[27–30] A frequent problem with small molecule inhibitors is the inadaquate specificity for thrombin with respect to other thrombolytic enzymes. A recent claim is that the interaction between Asp189 and a guanidine residue is not critical as previously thought: by replacing guanidine with methoxypropyl an enhancement of specificity for thrombin was realized.[24,31] It is noteworthy that nonenzymic functions of thrombin are not impaired in active-site blocked thrombin.

In the following, we wish to report on an application of the inhibition of thrombin that is different from those

discussed above: The inhibitors are a group of neutral phosphonate esters that provide reversibility of the catalytic activity. Reversible covalent modulation of thrombin activity could be of significant pharmaco-medical use because controllable release of thrombin, its mutant,[32] or its complex with a natural modifier, from a prodrug form, could improve the in vivo- and shelf-life of future formulations. Phosphonate esters provide greater diversity in physicochemical properties than the corresponding carboxyl esters due to higher valence states in P than in C. The physiologic properties of the anionic monophosphonate ester products are likely to be harmless.

Reversible modulation of thrombin activity has been investigated for 4-nitrophenyl 4-substituted phenacyl methylphosphonate ester (PMN; 4-CH_3-PMN; 4-CH_3O-PMN, see structures) inhibitors. The PMNs have a chiral center at the phosphorus atom. We have shown[33,34] earlier that serine proteases, particularly trypsin and chymotrypsin, prefer the levorotatory enantiomer over the dextrorotatory enantiomer. Since thrombin is a trypsin-like enzyme, it was expected that it would be inhibited by the PMN group of inhibitors and that it would prefer the levorotatory enantiomers. The enantioselectivity of thrombin for the three derivatives of PMNs has been found to be within 2–39 favoring the levorotatory enantiomers. As in the case of trypsin, chymotrypsin and t-PA, the inhibition of thrombin by PMNs is readily reversible due to carbonyl-participation in the dephosphonylation step.[33–35] The results of these studies are relevant to a potential medical use of temporarily phosphonylated thrombin.

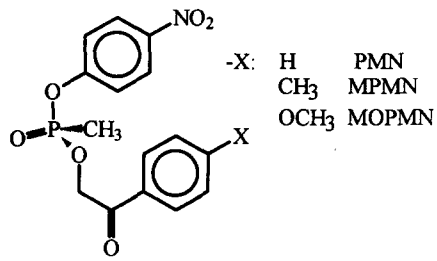

Results

Inactivation of thrombin by PMNs

The reaction between thrombin and the inhibitors can be described by the scheme below:

$$E + I \overset{K_i}{\rightleftharpoons} E^*I \overset{k_i}{\rightarrow} E' \qquad (1)$$

Since the initial concentration of the inhibitor, $[I_0]$, was at least 30-fold higher than the concentration of thrombin, the reaction was treated as pseudo first order. Background hydrolysis of the PMNs in pH 6.5, 0.025 M citrate buffer during the 2 or 3 min incubation times for inactivation at 7.0±0.1 °C, is below 5% and thus the approximation that inhibitor concentration [I] ~ $[I_0]$ seems acceptable. Expressing the observed rate constant in terms of Michaelis–Menten parameters and integrating the resulting differential equation[34,36,37] between limits $t = 0$, $[E] = [E_0]$ and for a given t, yields equation (2):

$$\ln\frac{[E_0]}{[E]} = \frac{k_i[I_0]}{K_i + [I_0]} \qquad (2)$$

The enzyme concentrations were linearly proportional to the initial rates of the hydrolysis of a fluorogenic substrate; $[v_0] \propto [E_0]$ and $[v] \propto [E]$, respectively. An average of three experimental $[v_0]/[v]$ ratios at each $[I_0]$ and at least four data pairs for a specific time increment were fit to the inverted form of equation (2):

$$\frac{1}{\ln\frac{[v_0]}{[v]}} = \frac{1}{k_i t} + \frac{K_i}{k_i t}\frac{1}{[I_0]} \qquad (3)$$

Statistical weighting was used in all cases. An example is given in Figure 1. The concentration range of the inhibitor used in the experiments was limited by solubility. Under the conditions, the slope giving the inverse of the second-order rate constant, k_i/K_i, was obtained with high precision but the intercept values yielding the inverse of k_i were not defined well. Since K_i was calculated from the ratio of the slope and intercept, the compounded errors in this parameter are the largest.

Rate constants k_i/K_i and k_i calculated for the inactivation of thrombin by the PMNs at pH 6.5 and 7.0±0.1 °C are presented in Table 1. Correction for buffer-catalyzed inhibitor hydrolysis had to be applied above pH 7.3. The time-dependent inhibitor concentration under these conditions can be expressed by $[I_o] \exp(-k_0 t)$, where k_0 is the first-order rate constant for hydrolysis. The corrected equivalent of equation (2) is given as

$$\ln\frac{[v_0]}{[v]} = \frac{k_i}{k_0}\ln\left(\frac{K_i + [I_0]}{K_i + [I_0]e^{-k_0 t}}\right) \qquad (4)$$

Equation (4) was used for fitting the data for inactivation of thrombin by PMN in the pL (L = H or D) range 7.4–8.4 in water, in the presence and absence of 0.15 M Na^+ ions, and in heavy water, respectively.

Figure 2 provides a graphical representation of the pL dependence of the second-order rate constants. The curves were calculated according to equation (5) with k_{obs} representing k_i/K_i.

$$k_{obs} = \frac{k_{lim1}K_a}{K_a + [H^+]} + k_{lim2} \qquad (5)$$

Kinetic pKs of 8.0±0.1 in 0.15 M NaCl and 7.4±0.1 in 0.15 M choline chloride, were calculated from the pH-dependent second-order rate constants, in water by using explicit errors. The pH-independent rate constants are $k_{lim1} = 2366\pm152$ M^{-1} s^{-1} and $k_{lim2} = 190\pm22$ M^{-1} s^{-1} in 0.15 M NaCl, and $k_{lim1} = 1490\pm188$ M^{-1} s^{-1} and $k_{lim2} = 77\pm63$ s^{-1} in 0.15 M choline chloride, respectively. The upper limit of k_i/K_i is 1048 ± 40 M^{-1} s^{-1}

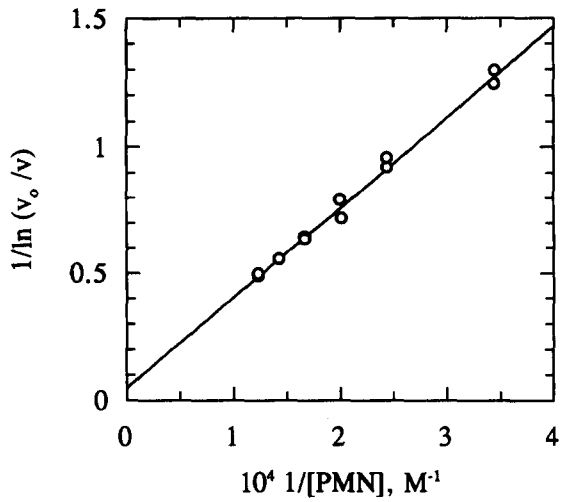

Figure 1. The inactivation of thrombin by (−)-PMN in 0.025 M citrate buffer pH 6.5, 0.15 M NaCl, 0.1% PEG-4000 at 7.0±0.1 °C.

in heavy water. The solvent isotope effect for the upper limit of the second-order rate constant, $^{DOD}k_i/K_i$, was calculated to be 2.26±0.17. Values are within 5% of the above when statistical errors were used in the calculation and the solvent isotope effect is 2.1±0.2. Due to the rapid competing hydrolysis of the inhibitors, the pH dependence of the k_i values could not be determined.

Reactivation of thrombin from the adducts with the PMN inhibitors

Lengthy experiments for the pH dependence of thrombin reactivation from adducts with the PMNs at

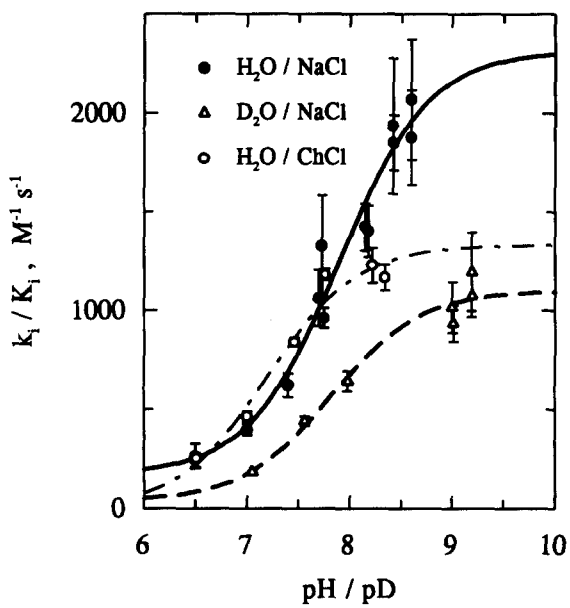

Figure 2. The pH dependence of the second-order rate constants for inactivation of thrombin with (−)-PMN in water in the presence of 0.15 M NaCl, in the presence of 0.15 M choline chloride and in the presence of 0.15 M NaCl in heavy water at 7.0±0.1 °C.

Table 1. Inactivation of thrombin by PMNs in 0.025M citrate buffer, 0.15 M NaCl, pH 6.5 at 7.0±0.1 °C. The rate constants are the mean values of two measurements

4-X-PMN	k_i/K_i (M^{-1} s^{-1})	10^2 k_i (s^{-1})	10^4 K_i (M)
-H (±)	124±4	23.0±14.4	18.5±11.1
-H (−)	234±8	19.0±13.0	8.8±6.1
-H (+)	6.5±0.9	0.63±0.17	10.7±1.65
$-CH_3$ (−)	57.7±4.7	1.13±0.13	1.90±0.20
$-CH_3$ (+)	7.3±1.2	0.32±0.03	4.30±0.72
$-OCH_3$(−)	53.4±9.2	0.34±0.09	0.63±0.17
$-OCH_3$(+)	21.7±2.5	0.51±0.04	2.35±0.25

25.0±0.1 °C had to be corrected from control experiments for a slight denaturation of thrombin shown in the scheme below;

$$[E_{inh}] \xrightarrow{k_r} [E] \xrightarrow{k_d} [E]^* \qquad (6)$$

where $[E_{inh}]$ is the initial concentration of inactivated thrombin, [E] is the concentration of free enzyme at time t, and k_r and k_d are the first-order rate constants for reactivation and enzyme denaturation, respectively. Recovering enzyme activity can be expressed by equation (7) where $[E_0]$ is the concentration of free enzyme at $t = 0$.

$$[E] = [E_{inh}]k_r\frac{e^{-k_r t} - e^{-k_d t}}{k_d - k_r} + [E_0]e^{-k_d t} \qquad (7)$$

The pH dependence of the reactivation rates of thrombin from adducts with (−)-CH_3-PMN and (−)-CH_3O-PMN was relatively small with kinetic pKs 7.27±0.11 and 8.22±0.10, respectively (statistical weighting). Rate constants were similar for the reactivation of thrombin from the adducts with enantiomers of PMN and from the adduct with (+)-CH_3-PMN: They were only slightly pH dependent. Figure 3 displays the fit of the data to equation (5) and Table 2 has the calculated parameters.

Computational results

Plausible starting structures were screened initially by minimization of conformations generated via rotation around the Ser195 C_α–C_β and P–OE bonds in the adducts. Those orientations were the most favorable, which allowed for interactions stabilizing the phosphoryl group with electrostatic or H-bonding forces, the methyl group and phenyl group of the phenacyl moiety

Table 2. pH-Independent rate constants and pK values for the reactivation of thrombin from its adducts with PMNs at 25.0±0.1 °C

4-X-PMN	pK_a	10^5 k_{lim1} (s^{-1})	10^5 k_{lim2} (s^{-1})
-H (−)	8.00±0.23	27.1±2.7	8.2±1.4
-H (+)	7.16±0.12	34.8±1.3	6.0±2.0
$-CH_3$ (−)	7.27±0.11	59.5±1.8	7.9±2.6
$-CH_3$ (+)	7.17±0.18	34.8±2.6	0.5±2.5
$-OCH_3$ (−)	8.22±0.10	79.5±3.9	13.9±1.9

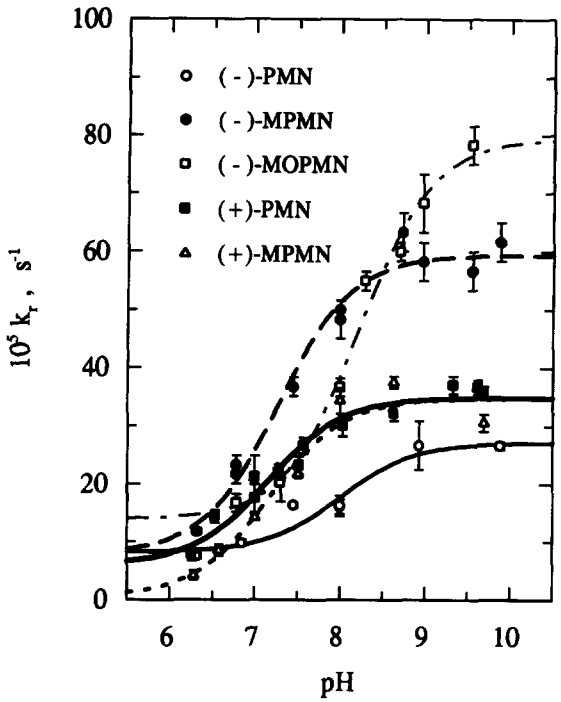

Figure 3. pH–Rate profiles for the reactivation of thrombin from its adducts with 4-substituted PMNs at 25.0±0.1 °C.

with hydrophobic regions, the carbonyl group of the phenacyl moiety with H-bond donors, and the substituent in the phenacyl moiety with polar groups on residues. Critical distances between inhibitor fragment and active-site residues are tabulated in Table 3 and Figures 4–6 provide the pictorial representation of the active-site interactions. Energy partitioning for the same interactions is given in Table 4.[38]

The phosphoryl oxygen of the P_S diastereomers[39] of the phosphonylated adducts of thrombin was accommodated in the oxyanion hole and stabilized by H-bonding to the HN of Gly193 and Ser195. It faced $HisH^+57$ and was bound to it by H-bonding and electrostatic interactions in the P_R diastereomers. Binding of the aromatic ring in the specificity pocket of thrombin was

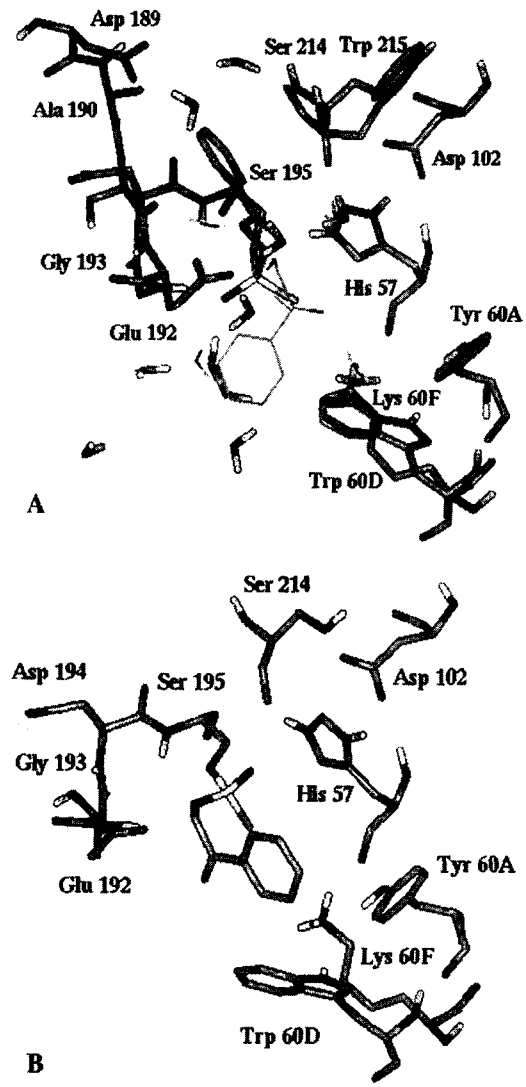

Figure 4. Active-site residues in the adducts of PMN-inhibited thrombin; **A.** P_S diastereomer with the aromatic ring in the binding pocket and the light line illustrates the mode of binding of the ring outside the pocket, **B.** P_R diastereomer. Atoms are distinguishable by the intensity of shading: in order of decreasing darkness are O, N, C, P, H.

Table 3. YETI-optimized structures of the (*R*)/(*S*)-4-X-PMN-thrombin adducts

	H			CH_3		OCH_3	
Interaction	(*R*)	$(S)_{out}$	$(S)_{in}$	(*R*)	(*S*)	(*R*)	(*S*)
His57Nδ–Asp102O	2.86	2.75	2.77	2.73	2.76	2.78	2.76
	(64)	(157)		(149)	(160)	(163)	(157)
His57Nε–InhOE	>5	2.71	3.01	4.82	2.72	2.73	2.71
	—	(146)		—	(148)	(146)	(146)
His57Nε–InhOP	2.97	5.00	5.02	2.68	5.01	4.93	5.01
	(80)	—		(141)	—	—	—
Gly193NH–InhOP	>5	2.79	2.80	4.89	2.78	2.55	2.78
	—	(149)		—	(147)	(131)	(148)
Ser195NH–InhOP	4.52	3.02	4.02	4.49	3.87	3.76	3.88
	—	(146)		—	(146)	(143)	(135)
Lys60FN–InhCO	>5	4.62	>5	>5	4.66	2.69	4.66

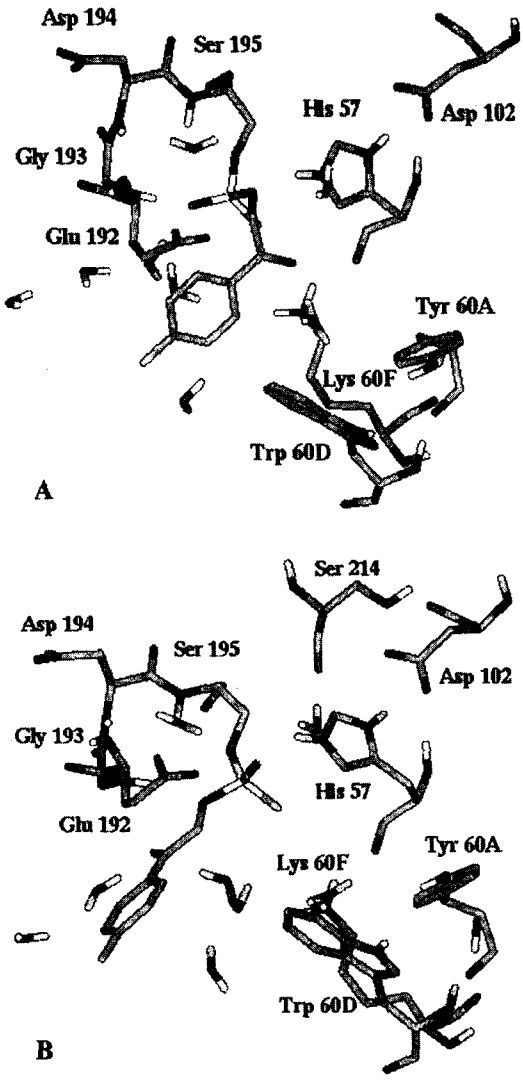

Figure 5. Active-site residues in the adducts of CH_3 PMN-inhibited thrombin; A. P_S diastereomer, B. P_R diastereomer. Atoms are distinguishable by the intensity of shading: in order of decreasing darkness are O, N, C, P, H.

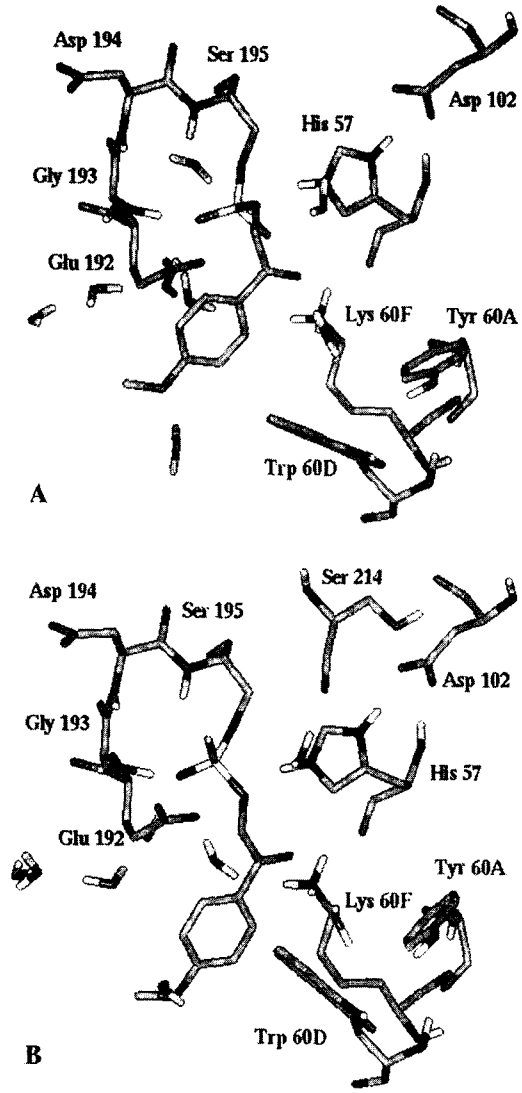

Figure 6. Active-site residues in the adducts of CH_3O PMN-inhibited thrombin; A. P_S diastereomer, B. P_R diastereomer. Atoms are distinguishable by the intensity of shading: in order of decreasing darkness are O, N, C, P, H.

possible only in the P_S adduct formed with PMN. The same adduct had another minimum-energy structure in which the aromatic ring was interacting with Trp60D of the loop region. The latter was the dominant mode of binding of the aromatic ring in all other adducts, partly due to steric constraints in the specificity binding region and partly due to conformational restrictions in the P_R diastereomers. The carbonyl group of the phenacyl moiety could be stabilized by electrostatic interactions with Lys60F and $HisH^+57$ in the P_S diastereomers.

Discussion

The purpose of this study was to evaluate the plausibility of reversible inhibition of human α-throm-

Table 4. Energy partitioning in the minimum-energy conformation of the 4-X-PMN-thrombin adducts

4-X-PMN	Total E kcal/mol	Prot–Inh kcal/mol	Wat–Inh kcal/mol	Inh–Inh kcal/mol	Sum kcal/mol
H (S) in	−8624.6	−47.5	−14.9	+4.3	−58.1
out	−8620.1	−39.1	−20.7	+1.8	−58.0
(R)	−8597.6	−35.9	−21.4	+0.5	−56.8
CH_3 (S)	−8620.1	−39.5	−21.8	+1.4	−59.9
(R)	−8613.1	−28.9	−26.1	+0.9	−54.1
OCH_3 (S)	−8624.2	−39.3	−26.0	+3.5	−61.8
(R)	−8623.3	−40.4	−21.2	+8.9	−52.7

bin with the PMN group of inhibitors and to characterize the mechanisms of enzyme inactivation and reactivation. We investigated and subsequently reported the unique propensity of the phenacyl group to participate in an intramolecular displacement of the active-site Ser from adducts of chymotrypsin, trypsin[33,35] and t-PA[34] covalently modified by the PMN group of inhibitors. In this study we found the intramolecular displacement also to be effective in diastereomers of PMN-inhibited thrombin. Differences in the rate of thrombin recovery can be interpreted from the energy-optimized structures of the covalent adducts.

Inactivation of thrombin by PMNs

The reaction of thrombin with the PMNs was as difficult to monitor as that of t-PA[34] and much more difficult to monitor than those of chymotrypsin and trypsin.[33] As the results indicate, the catalytic apparatus of thrombin can react effectively with three of the five PMN derivatives studied. Two derivatives, the 4-Cl and 4-NO_2-substituted phenacyl compounds, hydrolyze so rapidly[40] that the bimolecular reaction of trypsin-like enzymes is not competitive with them. The second-order rate constants for the inactivation of thrombin by PMN, CH_3-PMN and CH_3O-PMN are similar in magnitude to those for the inactivation of t-PA.[34] However, the levorotatory enantiomer of PMN reacted at least fourfold faster with thrombin than the other derivatives. This is in contrast with t-PA where no specificity was observed with the PMNs. The second-order rate constants for inactivation of trypsin[33] are between 230 and 880 M^{-1} s^{-1}.

In contrast, chymotrypsin was found to react with the PMNs two orders of magnitude faster than the trypsin-like enzymes.[33] This might be expected, since the two aromatic rings make the inhibitors very hydrophobic, which complies with the specificity of chymotrypsin for substrates. Thrombin and trypsin cleave peptide bonds at the carboxyl side of an Arg or Lys specifically. In general, there are more stringent specificity requirements in the blood cascade enzymes, including thrombin, than in trypsin.[2,21,41-44]

The binding of the PMNs to thrombin is somewhat weaker than to t-PA; K_i values for α-thrombin are in the μM range. Considering the efficient departure of the 4-nitrophenyl group, the k_i values probably measure the rate of P–O bond formation. Although precise values of k_i have not yet been reported for phosphonylation of the active-site Ser in serine hydrolases, our earlier results with t-PA were similar to the values measured for thrombin.[34] In contrast, acetylcholinesterase phosphonylation by 4-nitrophenyl esters of alkylphosphonates gave values 10–50 times higher at 25 °C than the k_i values for phosphonylation of thrombin.[36]

The solvent isotope effect of 2.26±0.17 is significant and indicative of proton transfer at the transition state of the phosphonylation step. A most likely origin of the solvent isotope effect is the proton removal by the active-site His57 from the attacking nucleophile, Ser195, on the phosphonate ester.

Enantioselectivity of thrombin for PMNs

The levorotatory enantiomers of PMNs inactivate thrombin preferentially as is the case with other serine proteases. PMN shows the greatest selectivity, 39-fold, for thrombin. As the size of the substituent in the para position of phenacyl increases, the selectivity decreases to ~2 in CH_3O-PMN.

Enantioselectivity up to 49 could be measured for the inactivation of trypsin by PMN, CH_3-PMN, and CH_3O-PMN.[33] The enantioselectivity of t-PA was not well established, but it seemed that the resolved (−)-enantiomer of CH_3-PMN inactivated t-PA at least ten times faster than the (+)-enantiomer of CH_3-PMN.[34] Overall the enantioselectivity of trypsin-like enzymes falls short of that of chymotrypsin (90–1900).

Reactivation of thrombin activity from the adducts with PMNs

The slowest and least pH-dependent recovery of thrombin is from the adduct formed with (−)-PMN. Thrombin reactivation from the adduct formed with (−)-CH_3-PMN is slightly faster and more pH-dependent than from the parent compound. The fastest recovery of thrombin activity is from the adduct with (−)-CH_3O-PMN, with approximately the same pH dependence as that from the adduct with (−)-CH_3-PMN. This is similar to that found with t-PA, and different from the fastest reactivating trypsin adduct, with (+)-CH_3-PMN.

The kinetic pK calculated from the data in Figure 3 for the adduct formed with (−)-CH_3O-PMN is 8.22 and similar to kinetic pKs reported for thrombin acylation by short substrates.[45] Reactivation of thrombin from (+)-PMN and (+)-CH_3-PMN proceeds at almost the same rate and gives almost identical pH profiles with kinetic pK values of 7.16 and 7.17, respectively. A change in the rate of dephosphonylation with the apparent ionization of an amino acid residue seems to indicate a transition between two somewhat different conformational states in the adducts formed with (−)-CH_3-PMN and (−)-CH_3O-PMN. Transition state stabilization is more effective in the conformation assumed after the loss of a proton. It appears that the residue affecting transition state stabilization is more buried and less solvated in the adduct formed with (−)-CH_3O-PMN because it has a unit higher pK than in the transition state of the other adducts. Release of the active-site Ser is especially difficult from the adducts with (−) or (+)-PMN and (+)-CH_3-PMN. Ionization of the residue has only a small effect on breaking the bond between P and SerOγ.

Computational results

Computational techniques were used previously in our interpretation of the molecular mechanisms of inhibition of serine hydrolase enzymes by phosphonate esters.[33,46–48] Reactions of thrombin have recently been interpreted in terms of interactions with residues surrounding the effector.[11–13] A hallmark of serine hydrolase activity in adducts with carboxyl and phosphoryl containing compounds seems to be the stabilization of the high electron density around these functional groups. The evolutionarily anticipated stabilizing force is the oxyanion hole providing two H-bond donors, Gly193 NH and Ser195 NH, at 3.05 and 2.80 Å from the carbonyl in the PPACK inhibited thrombin structure. Conjugates of noncovalent tripeptide methylester inhibitors of thrombin were recently compared with the analogous but covalently attached boronates.[13] The X-ray structures of these conjugates illuminated fine details of binding interactions in the conjugates: The protein structure was shown to adapt to the specific structural characteristics of a particular small molecule and to trade electrostatic interactions for hydrophobic interactions, or vice versa, in order to optimize binding. Some of the interactions described for the carbonyl and boronyl inhibitors are also significant in the P_S adducts of thrombin inhibited by PMNs; as the H-bonding distances in Table 3 indicate, Gly193 is the major H-bond donor to phosphonyl. The H-bond from Ser195 is weaker in all cases, because of the apparent intervention of a solvating water molecule above the plane of the H-bond to phosphoryl. In contrast, the phosphoryl moiety in the P_R adducts of thrombin inhibited by the PMNs faces $HisH^+57$ and is stabilized by electrostatic attraction. In fact, the minimum structure of this adduct has some unusual interactions: $HisH^+57$ is not aligned well with Asp102 or any of the oxygen proton acceptors of the phosphonylated Ser. Instead it interacts with the main-chain carboxyl of Ser214. The P_R adducts of thrombin with CH_3-PMN and CH_3O-PMN show the expected stabilizing interactions, an alignment between Asp102Oδ and $HisH^+57N\delta$ and one between $HisH^+57N\varepsilon$ and either the phosphoryl oxygen, in CH_3-PMN, or with the etheral oxygen of the phenacyl fragment, in CH_3O-PMN. These orientations of the catalytic His are reminiscent of the 'out' conformation in serine protease-catalyzed leaving group departure in the evolutionarily expected role of the enzymes.[49] There is a good H-bonding interaction between Gly193 and the phosphoryl oxygen in the P_R adduct of thrombin with CH_3O-PMN. It is tempting to suggest that the small stereoselectivity observed with enantiomers of CH_3O-PMN is consistent with negligible differences in the stabilizing interactions of the diastereomeric adducts. This is very similar to what has been observed with other phosphonate ester adducts of acetylcholinesterase.[46–48]

The methyl group of the phosphonate fragment binds in a fairly large hydrophobic region of the active site in every case. A key distinguishing element in stereoselectivity seems to be the phenacyl group. The aromatic ring finds ample opportunity for hydrophobic interactions with residues of the insertion loop, particularly Trp60D, in every structure. In one case, the P_S adduct of PMN-inhibited thrombin, the phenacyl ring lies perpendicular to the indole ring of Trp60D indicating a weak electrostatic interaction between two polarized aromatic entities.[50] There is also an equally low-energy structure for this diastereomer in which the ring is bound North of the insertion loop and interacts with the wall of the binding pocket of thrombin. It is not clear why the 4-substituted derivatives disfavor this orientation, but perhaps for steric interferences between the wall and the substituents. An ostensible difference between the diastereomers is in the binding of the carbonyl group: The electron-rich carbonyl is stabilized by Lys60F and even by $HisH^+57$ in the P_S diastereomers, while it is mostly solvated in the P_R diastereomers. Nevertheless, the carbonyl is available for the anchimeric assistance in catalyzing dephosphonylation of the enzyme in all cases. Because of the report on the versatility of the carboxylate side-chain of Glu192 in the binding of boronates, we considered a potential catalysis by Glu192 of water addition to the carbonyl of the phenacyl group. The conformation of the carboxyl side chain is not favorable for catalytic participation in this reaction.

The mechanism of reactivation of thrombin

The anchimeric assistance by the β-carbonyl group in the phenacyl ligand in phosphorus in the displacement of the active-site Ser from its phosphonate ester is the key to reversion of the inhibition of thrombin by these phosphonate esters. Scheme 1 shows details of the mechanism starting with a rapid general base-catalyzed hydration of the phenacyl group followed by the intramolecular attack of the anion of the carbonyl hydrate at the phosphorus reaction center and subsequent release of Ser195. The small pH dependence and small solvent isotope effects, ~1.2 for trypsin and chymotrypsin,[33] of reactivation suggest that proton transfer is not part of the rate-limiting process. Equation (8) gives the relationship of the observed rate constant to elementary rate constants;

$$k_{obs} = \frac{k'_h k_c}{k_{-h} + k_c}; \quad k_c = \frac{k_{obs} k_{-h}}{k'_h - k_{obs}} \tag{8}$$

In previous work, the hydration of carbonyl was found to be the rate-determining step in the mechanism of the nonenzymic hydrolysis of CH_3-PMN.[40] The 50% incorporation of ^{18}O from the medium is consistent with the contention that the rate constant for cyclization (k_c) is greater than for dehydration (k_{-h}). From the appropriate elementary rate constants and equilibria, this latter was estimated to be $\sim 10^6\ s^{-1}$. This value of k_{-h} is useful for a calculation of k_c in the enzymic reactions, because it is not expected to be sensitive to the differences in leaving group between CH_3-PMN and the corresponding Ser ester in the enzyme adduct. The value of k'_h is available from previous work for CH_3-PMN under a wide range of conditions and thus the

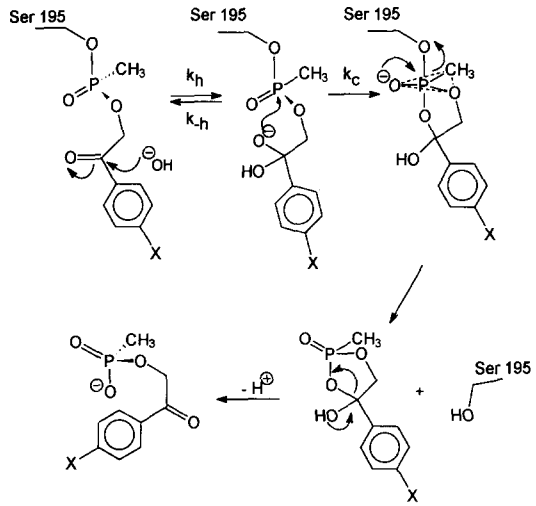

Scheme 1.

rate constant for cyclization (k_c) can be calculated using equation (8) for the reactivation of thrombin from the 4-methylphenacyl methylphosphonate adducts.

The calculation yields $k_c \sim 3.7 \times 10^4$ s^{-1} and is very similar to the value for trypsin, $k_c = 3.4 \times 10^4$ s^{-1}. These results indicate that the cyclization step is approx. 30 times slower than reversion of the carbonyl hydrate to starting materials. In comparison, $k_c = 10^5$ s^{-1} for t-PA, 1.2×10^5 s^{-1} for the reactivation of α-chymotrypsin from the adduct formed with the (+)-CH_3-PMN, and 4.5×10^3 s^{-1} for the reactivation of α-chymotrypsin from the adduct with the (−)-CH_3-PMN. *The rate of reactivation of thrombin is limited either by P–O bond breaking to Ser or by concerted displacement at P via cyclization.* This observation holds for serine protease reactivation from the adducts with the PMN group of inhibitors, except for the fastest reactivation of α-chymotrypsin from the adducts with CH_3-PMN and the (+)-enantiomers of PMNs.

Conclusions

Human α-thrombin can be efficiently inhibited by the PMN group of inhibitors at low temperatures when competing hydrolysis of the compounds is suppressed. The covalent attachment to thrombin involves weak binding of the small-molecule inhibitors, but rapid phosphonylation. The reversibility of the inhibition process can be modulated by the substituent in the phenacyl moiety. The rate of enzyme recovery from the three PMN derivatives at physiologic temperature is on the 2–7 h time scale and depends on the specific interactions between active-site components and effector. Thus these covalently modified thrombin adducts may have medical utility in pharmaceutical applications.

Experimental

Materials

Human α-thrombin (EC 3.4.21.5) was purchased from Enzyme Research Laboratories. N-*t*-Boc-Val-Pro-Arg 7-amido-4-methylcoumarin hydrochloride, 4-methylumbelliferyl-*p*-guanidinobenzoate hydrochloride (MUGB) and the HPLC grade solvents used in the separation of the enantiomers of PMNs were purchased from Sigma. The Chiracel OJ-7198 chiral column was purchased from J. T. Baker. Deuterium oxide (99.9 atom % D) was purchased from Aldrich. The phosphonate esters were synthesized as reported earlier.[40,51]

Separation of the enantiomers of PMNs by HPLC and quantitative analysis

The compounds were dissolved close to the saturation limit in the mobile phase, 65–70% 2-propanol and 35–30% *n*-hexane, at room temperature. The solutions were filtered using a 0.22 μm Cameo nylon filter. Repeated injections of 20 μL were performed. The operating conditions were 30 °C, flow rate 0.6 mL/min, and less than 500 psi pressure. The collected fractions were evaporated using a Yamato RE-51 rotary evaporator and redissolved in 500 μL dry acetonitrile. These stock solutions were stored at −70 °C. For quantitative analysis, 8 μL of inhibitor stock solution was added to 990 μL pH 7.2 0.05 M phosphate buffer, μ = 1 M (KCl) that had been preequilibrated at 25 °C. The stoichiometric equivalence of the ester was calculated from the absorbance due to the released *p*-nitrophenoxide, at 400 nm, upon hydrolysis. The time course of the hydrolysis reaction was recorded (ε = 9670 $M^{-1}cm^{-1}$) using a Perkin–Elmer Lambda-6 UV–vis spectrophotometer interfaced to a PC.

Enzyme activity assay

In the inactivation experiments the concentration of α-thrombin was determined by fluorometric active-site titration with 8.5 μM N-*t*-Boc-Val-Pro-Arg 7-amido-4-methylcoumarin hydrochloride[43] using an SLM-Aminco SPF-500C spectrofluorometer. All buffers were sterilized by filtration through 0.22 μm pore nylon filter. The assay buffer contained 0.05 M sodium barbital, 0.1 M NaCl and 0.1% PEG-4000 at pH 8.00. The release of 7-AMC was recorded (excitation 360 nm, emission 445 nm, concentration range up to 1.7 μM) in 0.4 s intervals for 20 s using a PC interfaced to the spectrofluorometer.

In the reactivation experiments, the concentration of thrombin was determined by fluorometric active site titration with MUGB[52] using the same assay buffer. The stoichiometric release of 4-MU was followed spectrofluorometrically (excitation 365 nm, emission 445 nm, concentration up to 30 nM). Data were recorded in 2 s intervals. The background hydrolysis of MUGB in the

assay buffer was recorded in advance for the same time period. Great care was taken to start the recording of the hydrolysis data beginning from the same reaction time as the titration, because these data were subtracted from the titration curve of thrombin.

Kinetics of inactivation

The inhibition was monitored at pH 6.5 in 0.025 M citrate buffer containing 0.15 M NaCl and 0.1% PEG-4000. Samples of 10–15 μL taken from the thrombin stock solution at 31.5 μM were diluted 100-fold with citrate buffer, vortexed and divided into 50 μL samples in 1.5 mL microcentrifuge tubes then equilibrated at 7.0±0.1 °C using a RTE-4 (NESLAB) circulating bath. The samples were kept on ice prior to inhibition. The stock solution of the inhibitor at 6–11 mM was prepared in dry acetonitrile and subsequently diluted with dry methanol. To each microcentrifuge tube were added 8–10 μL of the inhibitor solution at different concentrations save the control and the solution was mixed with a micro stirbar. Samples of 25 μL were taken at 2 and 3 min from the reaction mixture and were assayed for esterase activity. Duplicate experiments were performed for each reaction time and inhibitor concentration.

Kinetics of reactivation

Thrombin was inactivated by 0.10–0.25 mM (−)-PMNs at room temperature in 12–14 min until all excess of the inhibitor hydrolyzed.[40] The inhibition of thrombin with (+)-PMNs required ~1 mM concentration and was performed at ~4 °C for several hours to favor inhibition over hydrolysis. Reactivation was started by the addition of a buffer, which contained 20 mM Tris (pH 7.0–9.0) or Bis–Tris propane (pH 6.3–9.9), 0.15 M NaCl and 0.1% PEG-4000. The reaction mixture was then thermostated at 25.0±0.1 °C and kept under stirring. Samples of 15, 20, and 25 μL were drawn at 7–20 min intervals to be assayed for thrombin activity. Control runs for thrombin activity under conditions of the experiments were carried out the same way. Calculation of the rate constants and other data reduction were performed with program GraFit 3.0.[53]

Solvent isotope effects

Inhibition experiments using (−)-PMN were done at 7.0±0.1 °C in the 6.5–8.6 pH range using 0.025 M phosphate buffer, 0.15 M NaCl, and 0.1% PEG-4000. Buffers were prepared by weight in water and heavy water. The pD of the buffers in heavy water was calculated by adding 0.4 to the reading of the (Radiometer) pH meter.[54–56] The kinetic protocol was identical in the isotopic buffers.

Computational studies

Starting structure. The X-ray crystallographic coordinates of PPACK-inhibited α-thrombin (1.9 Å resolution) were retrieved from the Brookhaven Protein Data Bank.[7,10] The inhibitor and the labels designating the two chains of α-thrombin were removed from the data file. The positions of polar hydrogen atoms were assigned using the utility program HYDPOS in the YETI (5.3) molecular mechanics package.[33,46,48,57] In the YETI force-field hydrogen atoms attached to carbon atoms are represented as 'united' atoms. Acidic and basic residues were given unit electrostatic charge. All Tyr and Cys residues were neutral. The site of protonation of the His residues were based on the availability of H-bond donors or acceptors. His57 was protonated on both nitrogens Nε and Nδ to correspond to the results of NMR pH-titrations of phosphorylated adducts of trypsin and chymotrypsin[58,59] and the neutron diffraction data of monoisopropylphosphoryl-trypsin.[60] AUTOSOL was used for generating one water shell around thrombin. From the newly generated water molecules only those were accepted which were H-bonded to the protein.

Adduct fragments. The atom-centered charges were calculated by the semiempirical method MNDO as implemented in MOPAC and reported earlier.[33] The active-site Ser195 was modified with the desired fragment. Structures were constructed for the P_R and P_S diastereomers of the tetracoordinate adducts of thrombin with the PMNs.

Molecular mechanics simulations. The solvated structure without the adduct fragment was first energy minimized. Then the adduct fragment was attached and a conformational analysis was performed manually as follows: the fragment was rotated by 10° increments for a full circle around the Ser195 C_α–C_β bond and then the best structure was used for a second full circle rotation around the P–OE bond. Molecular mechanics calculations were performed with YETI (5.3):[57] The conformation of the main chain remained unaltered and only torsions were calculated from the bonded interactions. Van der Waals (vdW) and electrostatic contributions were computed for all non-bonded pairs. In addition, hydrogen bonds (Hb) were calculated with a 10/12 potential and angular dependence. The minimization was performed step-wise and a distance dependent dielectric parameter $D(r) = 2r$ was used. First a crude minimization was run on the adduct fragment and water molecules only using the steepest descent method (SD) and the following on/off cutoff values (Å) for interactions: electrostatic 5.5/6.0, vdW 4.5/5.0, Hb 3.5/4.0. The upcoming minimization steps allowed for longer cutoff values and smaller energy gain/cycle and were performed on larger zones around the inhibitor. The final refinement included a 15 Å zone around the inhibitor, allowed for 0.05 kcal/mol gain in energy and used the following cutoff values (Å) for interactions: electrostatic 9.5/11.5, vdW 7.0/9.0, Hb 4.5/6.5.

Acknowledgements

This research was supported by a Grant-in-Aid from the American Heart Association.

References

1. Dang, Q. D.; Vindigni, A.; Di Cera, E. *Proc. Natl. Acad. Sci. U.S.A.* **1995**, *92*, 5977.

2. Stubbs, M. T.; Bode, W. *TIBS* **1995**, *20*, 23.

3. Parry, M. A. A.; Stone, S. R.; Hofsteenge, J.; Jackman, M. P. *Biochem. J.* **1993**, *290*, 665.

4. Abbreviations: 7-AMC, 7-amino(amido)-4-methylcoumarin; Bis–Tris propane, 1,3-bis[tris(hydroxymethyl)methylamino]-propane; Chiracel-OJ, cellulose tri-4-methyl-benzoate coated silica; Hb, hydrogen bond; MNDO, minimum neglect of differential overlap; 4-MU, 4-methylumbelliferone; MUGB, 4-methylumbelliferyl-*p*-guanidinobenzoate hydrochloride; PEG-4000, polyethylene glycol (MW 4000); PMNs, 4-nitrophenyl 4-X-substituted-phenacyl methylphosphonates; pNP, 4-nitrophenol; t-PA, tissue-type plasminogen activator enzyme; Tris, Tris-(hydroxymethyl)-aminomethane; vdW, van der Waals.

5. Davie, E. W.; Fujikawa, K.; Kisiel, W. *Biochemistry* **1991**, *29*, 10363.

6. Bode, W.; Huber, R.; Rydel, T. J.; Tulinsky, A. In *Thrombin: structure and function*; Berliner, L. J., Ed.; Plenum: New York, 1992; Chapter 1.

7. Bode, W.; Mayr, I.; Baumann, U.; Huber, R.; Stone, S. R.; Hofsteenge, J. *EMBO J.* **1989**, *8*, 3467.

8. Bode, W.; Stubbs, M. T. *Semin. Thromb. & Hemost.* **1993**, *19*, 321.

9. Rezaie, A. R. *Biochemistry* **1996**, *35*, 1918.

10. Bode, W.; Turk, D.; Karshikov, A. *Protein Sci.* **1992**, *1*, 426.

11. Katakura, S.; Nagahara, T.; Hara, T.; Iwamoto, M. *Biochem. Biophys. Res. Commun.* **1993**, *197*, 965.

12. Rehse, P. H.; Steinmetzer, T.; Li, Y.; Konishi, Y.; Cygler, M. *Biochemistry* **1995**, *34*, 11537.

13. Nienaber, V. L.; Mersinger, L. J.; Kettner, C. A. *Biochemistry* **1996**, *35*, 9690.

14. Di Cera, E.; Hopfner, K.-P.; Dang, Q. D. *Biophys. J.* **1996**, *70*, 174.

15. Dunwiddie, C.; Thornberry, N. A.; Bull, J. G.; Sardana, M.; Friedman, P. A.; Jacobs, J. W.; Simpson, E. *J. Biol. Chem.* **1989**, *264*, 16694.

16. DeCristofaro, R.; Fenton, J. W.; Dicera, E. *Biochemistry* **1992**, *31*, 1147.

17. Di Cera, E.; DeCristofaro, R.; Albright, D. J.; Fenton, J. W. *Biochemistry* **1991**, *30*, 7913.

18. Wells, C. M.; Di Cera, E. *Biochemistry* **1992**, *31*, 11721.

19. Guinto, E. R.; Di Cera, E. *Biochemistry* **1996**, *35*, 8800.

20. Dang, Q. D.; Di Cera, E. *Proc. Natl. Acad. Sci. U.S.A.* **1996**, *93*, 10653.

21. Das, J.; Kimball, S. D. *Bioorg. Med. Chem.* **1995**, *3*, 999.

22. Jetten, M.; Peters, A. M.; Grootenhuis, P. D. J.; Van Nispen, J. W.; Ottenheijm, H. C. J. *Bioorg. Med. Chem.* **1995**, *3*, 1099.

23. Lienhard, G. E. *Science* **1973**, *180*, 149.

24. Tapparelli, C.; Metternich, R.; Ehrhardt, C.; Zurini, M.; Claeson, G.; Scully, M. F.; Stone, S. R. *J. Biol. Chem.* **1993**, *268*, 4734.

25. Claeson, G.; Philipp, M.; Agner, E.; Scully, M. F.; Metternich, R.; Kakkar, V. V.; Desoyza, T.; Niu, L.-H. *Biochem. J.* **1993**, *290*, 309.

26. Elgendy, S.; Deadman, J.; Patel, G.; Green, D.; Chino, N.; Goodwin, C. A.; Scully, M. F.; Kakkar, V. V.; Claeson, G. *Tetrahedron Lett.* **1992**, *33*, 4209.

27. Oleksyszyn, J.; Boduszek, B.; Kam, C.-M.; Powers, J. C. *J. Med. Chem.* **1994**, *37*, 226.

28. Bertrand, J. A.; Oleksyszyn, J.; Kam, C.-M.; Boduszek, B.; Presnell, S.; Plaskon, R. R.; Suddath, F. L.; Powers, J. C.; Williams, L. D. *Biochemistry* **1996**, *35*, 3147.

29. Goodwin, C.; Deadman, J.; Green, D.; Cheng, L.; Scully, M. F.; Kakkar, V. V.; Claeson, G. *Thromb. Haemost.* **1993**, *69*, 667.

30. Odake, S.; Kam, C. M.; Powers, J. C. *J. Enzym. Inhib.* **1995**, *9*, 17.

31. Tapparelli, C.; Metternich, R.; Ehrhardt, C.; Cook, N. S. *Trends Pharmcol. Sci.* **1993**, *14*, 366.

32. Gibbs, C. S.; Coutre, S. E.; Tsiang, M.; Li, W.-X.; Jain, A. K.; Dunn, K. E.; Law, V. S.; Mao, C. T.; Matsumura, S. Y.; Mejza, S. J.; Paborsky, L. R.; Leung, L. L. K. *Nature (London)* **1995**, *378*, 413.

33. Zhao, Q.; Kovach, I. M.; Bencsura, A.; Papathanassiu, A. *Biochemistry* **1994**, *33*, 8128.

34. Zhao, Q.; Kovach, I. M. *Bioorg. Med. Chem.* **1996**, *4*, 523.

35. Kovach, I. M.; McKay, L. *Bioorg. Med. Chem. Lett.* **1992**, *2*, 1735.

36. Kovach, I. M. *J. Enzym. Inhib.* **1991**, *4*, 201.

37. Hogg, P. J.; Jackson, C. M. *Proc. Natl. Acad. Sci.* **1989**, *86*, 3619.

38. All interaction energies were calculated under completely identical conditions with the same number of solvate water for each enzyme. The protein–protein interactions were essentially unchanged from structure to structure, and water–water and protein–water interactions varied very little. Thus, the differences in interaction energies were completely related to the interactions of the fragment with the protein and water environment. Although calculation of free energy perturbation may be considered the most rigorous method of evaluation of relative stabilities of the adducts, the structures compared in this work are structural isomers or close analogues which should lend credence to the data analysis.

39. Note that in-line displacement of 4-nitrophenol by serine causes no change in notation of the configuration around P because 4-nitrophenol has the highest priority in the reactant, but serine is only second in priority in the adduct.

40. Kovach, I. M.; Zhao, Q.; Keane, M.; Reyes, R. *J. Am. Chem. Soc.* **1993**, *115*, 10471.

41. Lottenberg, R.; Hall, J. A.; Blinder, M.; Binder, E. P.; Jackson, C. M. *Biochim. Biophys. Acta* **1983**, *742*, 539.

42. Kawabata, S.; Miura, T.; Morita, T.; Kato, H.; Fujikawa, K.; Iwanaga, S.; Takada, K.; Kimura, T.; Sakakibara, S. *Eur. J. Biochem.* **1988**, *172*, 17.

43. Morita, T.; Kato, H.; Iwanaga, S.; Takada, K.; Kimura, T.; Sakakibara, S. *J. Biochem.* **1977**, *82*, 1495.

44. DiBella, E. E.; Scheraga, H. A. *Biochemistry* **1996**, *35*, 4427.

45. Stone, S. R.; Betz, A.; Hofsteenge, J. *Biochemistry* **1991**, *30*, 9841.

46. Bencsura, A.; Enyedy, I.; Viragh, C.; Akhmetshin, R.; Kovach, I. M. In *Enzymes of The Cholinesterase Family*; Quinn, D. M., Balasubramanian, A. S., Doctor, B. P., Taylor, P., Eds; Plenum: New York, 1995; pp 155–162.

47. Bencsura, A.; Enyedy, I.; Kovach, I. M. *Biochemistry* **1995**, *34*, 8989.

48. Bencsura, A.; Enyedy, I.; Kovach, I. M. *J. Am. Chem. Soc.* **1996**, *118*, 8531.

49. Bizzozero, S. A.; Dutler, H. *Bioorg. Chem.* **1981**, *10*, 46.

50. Burley, S. K.; Petsko, G. A. *Science* **1985**, *229*, 23.

51. Lieske, C. N.; Mejza, S. J.; Steinberg, G. M.; Pikulin, J. N.; Lennox, W. J.; Ash, A. B.; Blumbergs, P. *J. Agric. Food Chem.* **1969**, *17*, 255.

52. Jameson, G. W.; Rooberts, D. V.; Adams, R. W.; Kyle, W. S. A.; Elmore, D. T. *Biochem. J.* **1973**, *131*, 107.

53. Leatherbarrow, R. J.*GraFit*; Erithacus Software Ltd., U. K. 1992; pp 1–288.

54. Schowen, R. L.; Schowen, K. B. *Meth. Enzymol.* **1982**, *87*, 551.

55. Venkatasuban, K. S.; Schowen, R. L. *CRC Crit. Rev. Biochem.* **1985**, *17*, 1.

56. Quinn, D. M.; Sutton, L. D. In *Enzyme Mechanism from Isotope Effects*; Cook, P. F., Ed.; CRC: Boston, MA, 1991; pp 73–126.

57. Vedani, A. J.; Huhta, D. W. *J. Am. Chem. Soc.* **1990**, *112*, 4759.

58. Porubcan, M. A.; Westler, W. M.; Ibanez, I. B.; Markley, J. L. *Biochemistry* **1979**, *18*, 4108.

59. Markley, J. L.; Neves, D. E.; Westler, W. M.; Ibanez, I. B.; Porubcan, M. A.; Baillargeon, M. W. *Developmental Biochemistry* **1980**, *10*, 31.

60. Kossiakoff, A. A.; Spencer, S. A. *Biochemistry* **1981**, *20*, 6462.

(*Received in U.S.A.* 9 *January* 1997; *accepted* 26 *March* 1997)